



Structural properties of shear zone materials of the Neogene soft-rock landslides in the northeastern margin of the Tibetan Plateau

Peng Xin¹ · Liangqing Wang² · Zhen Liu^{3,4} · Tao Wang¹ · Shu-ren Wu¹

Received: 12 January 2020 / Accepted: 20 April 2021 / Published online: 26 April 2021
© Springer-Verlag GmbH Germany, part of Springer Nature 2021

Abstract

Seven landslides among the 110 landslides on the northeastern margin of the Tibetan Plateau in China were selected to analyze the structural development processes within the shear zones. In addition, the platy clay mineral content and mineralogical composition of the shear zone were also investigated. The samples obtained from the vertical profiles were quantitatively studied from top to bottom with respect to their material composition, pore structure, and water properties to understand the changes in the cementation and frictional properties of the shear zone. The results indicate that the structure is progressively modified by fractures, cleavage, and plasticization. Even though there is no sliding surface liquefaction, clayey particles are observed to exhibit slipping and rearrangement. The illite–montmorillonite mixed-mineral layer accumulates near sliding surface in the core zone, and the platy clay minerals are arranged along shearing direction for long shear displacement.

Keywords Neogene soft rock · Shear zone · Clay minerals · Structural characteristics

Introduction

Neogene soft rock is widely distributed in the northeastern margin of the Tibetan Plateau in China and in the Duero Basin in Spain (Caterina et al. 2010, 2013; Yenes et al. 2009, 2015). Several landslides have occurred in this type of rock groups. A typical shear zone in the Neogene soft rock includes two groups of horizontal boundary faults and several internal secondary shear planes (Hart 2000; James 2001). The clay mineral content in the Neogene soft-rock shear zones is greater than 30% (e.g., Xin et al. 2018;

Yenes et al. 2009, 2015). Picarelli et al. (2006) observed specimens exhibiting small shear fissures, which can be observed as groups of shear structures exhibiting similar orientations in hard-soil shear zones. The structural development characteristics of the shear zones would change gradually during large shear displacement. Therefore, a detailed study of shear zone development is considered to be crucial for understanding the development of landslides in the case of Neogene soft rocks.

The deformation behavior of the shear zone during large shear displacement is an important factor associated with mass movements involving residual and steady-state strength. Skempton (1985) observed the development of a low-angle failure surface in pure montmorillonite and illite, with the internal friction angles reaching 5° and 10°, respectively. Lupini et al. (1981) observed that the occurrence of horizontal faults in London clay can be determined based on its clay content under drained shear tests with a displacement of lower than 100 cm (Fig. 1a–c). When the clay content was greater than 40%, a 1.5-mm-thick shear zone was parallel to the shear direction (Fig. 1b). However, two sets of shear planes can be clearly observed when the content of clay was greater than 48%. The shear zone is approximately 2.5-mm thick, and the angle between the clay mineral orientation and shear

✉ Zhen Liu
zliu@thompsonengineering.com; zhenliu.ce@gmail.com

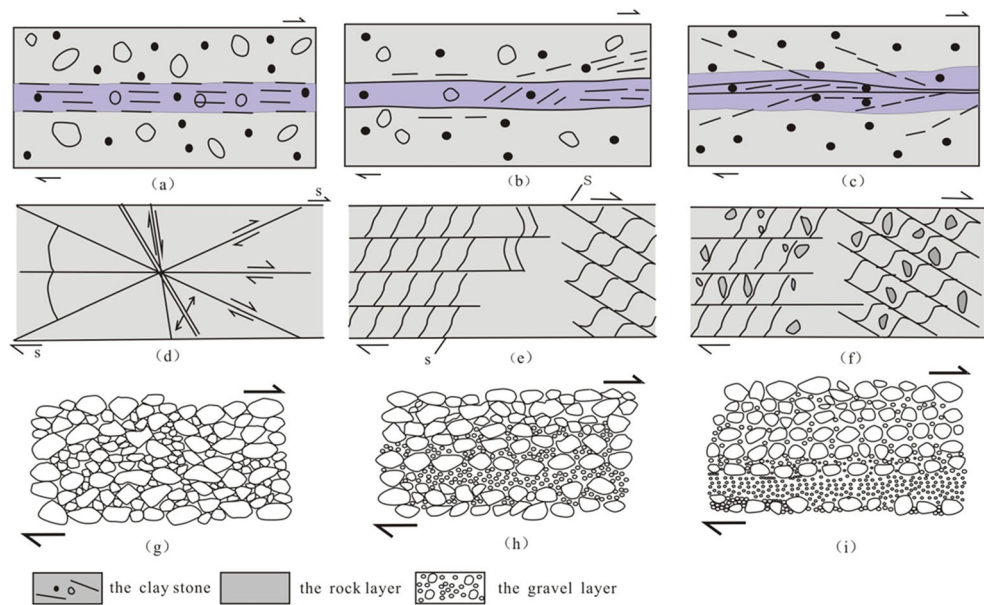
¹ Key Laboratory of Neotectonic Movement and Geohazards, Ministry of Land and Resources, Institute of Geomechanics, Chinese Academy of Geological Sciences, Beijing 100081, China

² Faculty of Engineering, China University of Geosciences, Wuhan 430074, China

³ Formerly the Department of Civil & Environmental Engineering, Louisiana State University, Baton Rouge, LA 70803, USA

⁴ Thompson Engineering, Baton Rouge, LA 70816, USA

Fig. 1 Mechanical modeling of the shear zone and rearrangement of the internal clay minerals (Lupini et al. (1981), Yenes et al. (2009), and Muhammad et al. (2004)): **a** cataclastic failure with a clay fraction of 34%; **b** cataclastic failure with a clay fraction of 40%; **c** cleavage failure with a clay fraction of 48%; **d** Riedel shear fracture with high calcium carbonate content; **e** ductile shear fracture with an abundant amount of clay; **f** ductile–brittle fracture; **g** initial structure of a sandy shear zone; **h** progressive rupture of a sandy shear zone; and **i** layered deposition of particles



direction is $<45^\circ$ (Fig. 1c). Yenes et al. (2009) considered that the shear zone, including the boundary fault planes, central shear planes, and a Riedel plane with high calcium carbonate content, exhibited brittle failure in accordance with the Riedel shear criterion (Fig. 1d). The boundary faults and cleavage planes could be observed in a ductile shear zone comprising an abundant amount of clay (Figs. 1e–f). The particles in the shear zone will be arranged in layers when the shear displacement in the shear zone increases from 20 cm to 10 m (Muhammad et al. 2004; Wang et al. 2000). For example, when silica sand was continually sheared, the grain size decreased and the thickness of the core zone reduced from 4 to 2.2 cm; fine particles were observed to be concentrated near the slip surface (Fig. 1i) (Muhammad et al. 2004). Picarelli et al. (2006) believed that the platy clay minerals in the core zone would be arranged along a plane parallel to the shear plane and that the content of these minerals would continually increase under continuous shearing. However, the relation between the mineral content and water in any region of the Neogene soft-rock shear zone, which comprises clay particles, has not been addressed. Quantitative analysis of a geological section would be beneficial to reveal the development processes in the slide mass.

The distribution characteristics of clay minerals are crucial to understand the development of the Neogene soft-rock shear zones. Previously, the ring shear tests were conducted to investigate the evolution of the shear zone structure (e.g., Lupini et al. 1981; Wang et al. 2000). However, the confining pressure and shear displacement in experiment cannot reach the values obtained in situ in case of landslides (Carey and Petley 2014; Skempton 1970; Xin et al. 2016, 2018). To address these discrepancies, the distribution characteristics of clay minerals and the exchange

process between clay minerals and pore water in case of actual landslides were investigated.

Geological profiles and testing methods

Seven landslides among the 110 landslides on the northeastern margin of the Tibetan Plateau in China were selected to analyze the distribution of clay minerals and their interaction with water (e.g., Xin et al. 2016, 2018). These landslides can be divided into two groups, i.e., short-distance landslides with a movement distance of less than 100 m (such as Caijiapo landslide and Songjiayao landslide) and long-distance landslides with a movement distance of more than 100 m (such as Bojishan landslide, Gaojiaya landslide, Caizigou landslide, Xinguancun landslide, and Liujiashuang landslide).

Geological profile and structure

The shear zones are characterized by layers exhibiting cataclasis, cleavage, and argillation in the core and are described below.

Cataclastic layer The cataclastic layers in shear zones are in the initial stage of failure, and their structure is consistent with the Riedel fracturing. The sliding zone of the Caijiapo landslide, which occurred in 1932, is approximately 0.8-m thick and 320-m long. The shear zones of the Caijiapo landslide (Fig. 2(a) and (b)) and the Songjiayao landslide (Fig. 2(c) and (d)) comprise two sets of boundary faults and central shear planes, above which a cataclastic zone can be observed.

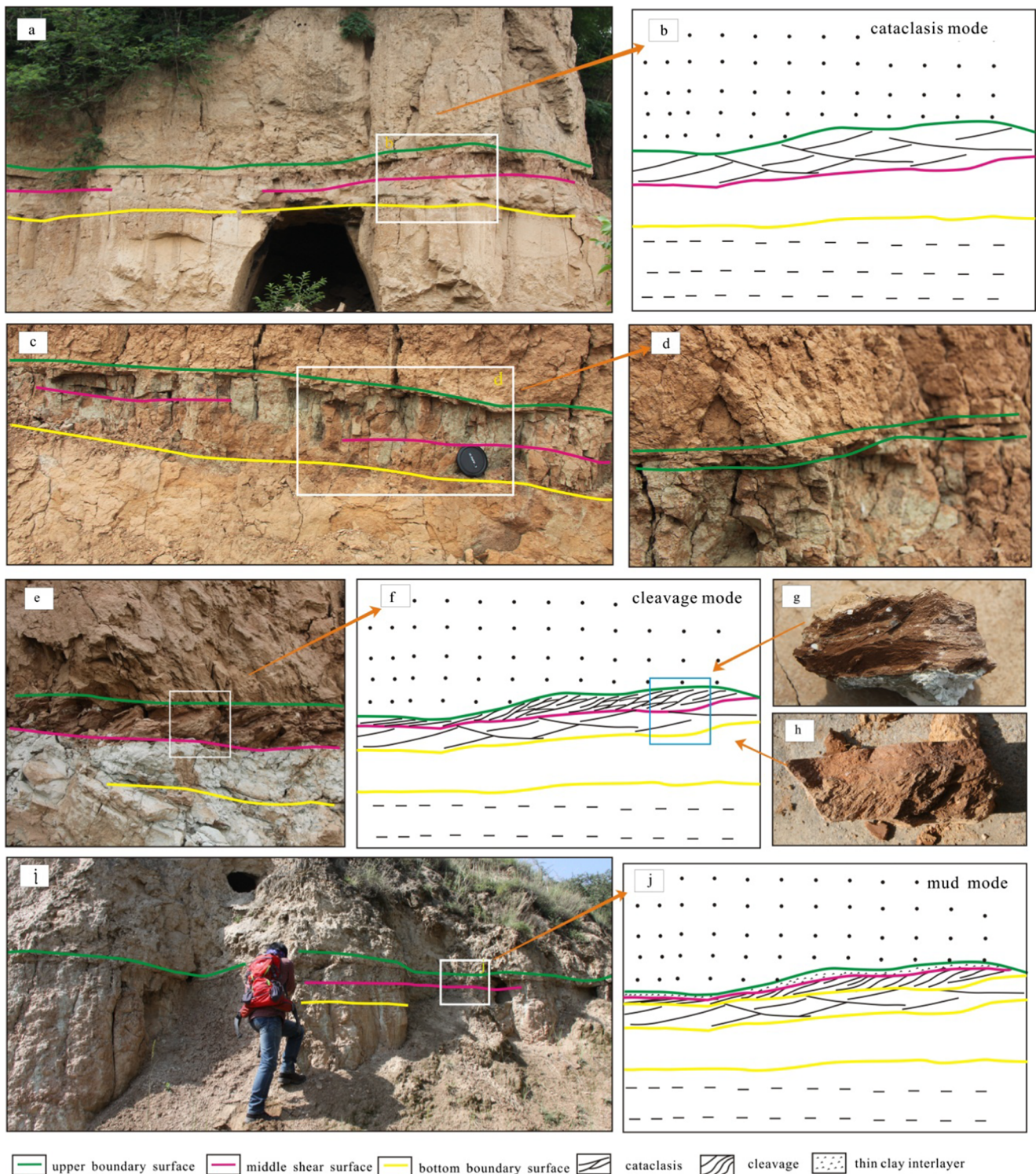


Fig. 2 Photos and geological profiles of the shear zone in landslides considered in this study. a–b cataclastic structures in shear zone of Caijiapo landslide; c–d photos of the shear zone in Songjiayao landslide;

e–h cleavage structures in shear zone of Liujiazhuang landslide; i–j plastic structures in shear zone of Caizigou landslide

Cleavage layer In the cleavage layer, clay minerals are arranged in a network comprising individual or stacked plates and are characterized with bright and reflective layers that may exhibit scratches in the core. The slip zone

is approximately 0.6-m thick in the Liujiazhuang landslide. Plastic and cleavage zones developed near the upper shear plane, with a spacing of less than 0.2 cm between the cleavage planes (Fig. 2(e) and 2(f)). Similar features can

also be observed in the Gaojiaya landslide (Fig. 2(g) and 2(h)).

Argillaceous layer In the argillaceous layer, the soft rock has undergone weathering, and the cementation structure is completely deteriorated. The observed structure comprises powdered particles that have undergone plastic deformation in fairly thin layers. A film of water has also been observed on some of the shear planes. For example, in the Caizigou landslide, the thicknesses of the mud layer, cleavage zone, and cataclasis slip zone are approximately 2 cm, 0.3 m, and 0.75 m, respectively.

Testing methods and procedures

The cumulative displacements of the core and boundaries of the shear zones are different and exhibit different characteristics (Muhammad et al. 2004; Wang et al. 2000). The vertical profiles in Fig. 3 were quantitatively studied from top to bottom in terms of the material composition, pore structure, and water properties of each sample location to understand the changes in the structure of the shear zone. Testing proceeded via three steps after the onsite borehole drilling. The first step

involved the preparation of thin sections from samples along the vertical profile of core. Subsequently, the mineral content and the arrangement of minerals at each position were determined using a polarizing microscope. Step two includes testing the quantitative characteristics of the clay minerals, pore structure, and water content along the identified shear zone. Finally, the sliding process of the unsaturated samples under undrained conditions and long shear displacement were analyzed.

Fifty samples are selected for testing from among six geological profiles with different forming times and stress environments. The sample core ZK1 from the Caizigou landslide, cores ZK3 and ZK4 from the Xinguncun landslide, and core ZK2 from the Bojishan landslide were obtained from the center of their respective landslide masses. The sampling interval in ZK1 (Caizigou landslide) was in the range of 1–6 m, as shown in Fig. 3a. For ZK3 and ZK4 (Xinguncun landslide), samples were obtained at intervals of 0.5–2 m, as shown in Fig. 3b. Figure 3c shows the sampling scheme at an interval of 0.1–0.2 m for ZK2 (Bojishan landslide). The horizontal shear zones are prominently exposed in the contraction zones of the front edge of a translational sliding body. Because of the good accessibility of such zones in the Liujiazhuang, Gaojiaya, and

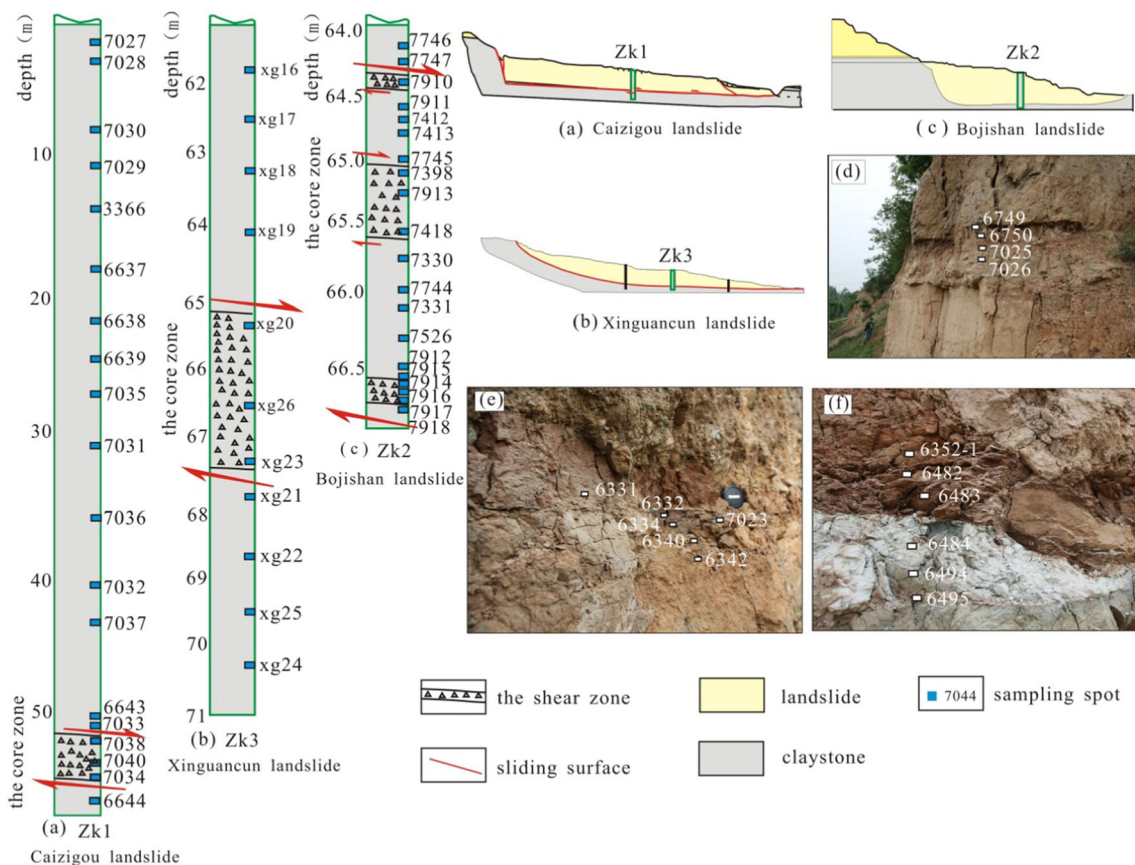


Fig. 3 Sampling in landslides from the northeastern margin of the Tibetan Plateau: **a** borehole ZK1 in the Caizigou landslide; **b** borehole ZK3 in the Xinguncun landslide; **c** borehole ZK2 in the Bojishan

landslide; **d** sampling of the Caijiapo landslide; **e** sampling of the Gaojiaya landslide; and **f** sampling of the Liujiazhuang landslide

Table 1 Sample composition and clay mineral data from the shear zones at the foot of landslides

Location	Sampling number	Water content (%)	Plastic index (%)	Particle size <0.002 mm content (%)	Specific surface area (m ² /g)	Montmorillonite in mixed layer (%)	Calcium carbonate content (%)	Relative content of clay minerals (%)			Mixed-mineral layer ratio (%)			Absolute content of clay minerals (%)				
								S	I/S	I	K	C	S	I/S	I	K	C	
Caizigou landslide with an argillaceous layer																		
	7034	24.08	27.75	39.64	232.74	26.26	4.23	/	59	25	7	9	65	/	24.6	10.4	2.9	3.8
	7038	25.74	23.70	28.20	205.66	20.34	6.27	/	54	27	8	11	55	/	20.0	10.0	3.0	4.1
Bojishan landslide with an argillaceous layer																		
Core zone	7910	28.82	29.54	62.60	250.55	29.23	1.36	/	69	21	7	6	80	/	50.1	13.2	4.4	3.8
	7914	25.52	27.99	58.04	224.14	27.31	1.18	/	69	22	5	4	65	/	40.1	12.8	2.9	2.3
Caijiapo landslide with cataclastic layers																		
	6749	/	27.79	50.36	211.09	25.29	11.00	/	73	19	5	3	65	/	36.8	9.6	2.5	1.5
Core zone	6750	/	22.78	39.80	168.68	22.78	4.77	/	67	24	5	4	75	/	26.7	9.6	2.0	1.6
Core zone	7025	/	22.08	34.08	240.99	23.23	2.21	/	67	23	5	5	75	/	23.2	8.0	1.7	1.7
Gaojiaoya landslide with a cleavage layer																		
	6331	10.38	19.65	23.84	121.05	11.53	9.71	/	59	26	7	7	59	/	14.0	6.2	1.6	1.9
	6332	16.76	19.85	38.19	156.22	19.05	/	/	67	26	7	67	67	/	25.5	9.9	2.6	2.6
Core zone	6334	17.14	20.36	31.89	168.10	18.87	8.16	/	75	14	6	6	75	/	23.9	4.4	1.9	1.6
Core zone	7023	/	22.51	25.72	199.81	18.96	22.14	/	69	20	5	6	75	/	19.1	5.6	1.4	1.7
	6340	/	19.36	27.60	108.00	7.00	2.00	/	82	12	6	6	45	/	22.6	3.3	1.6	1.6
	6342	/	22.07	27.49	165.93	21.47	0.35	/	75	15	7	7	55	/	28.4	5.6	2.6	2.0
Liujiashuang landslide with a cleavage layer																		
	6352-1	20.22	19.71	29.90	90.12	10.26	3.26	/	59	25	7	9	55	/	28.4	5.6	2.6	1.1
Core zone	6482	16.16	22.83	38.48	262.9	25.46	4.71	/	78	18	4	2	55	/	29.2	6.9	1.5	0.7
Core zone	6483	15.56	22.48	31.87	214.1	20.02	6.64	/	69	21	6	4	40	/	21.9	6.6	1.9	1.2
	6484	14.75	20.35	28.99	226.9	18.49	9.00	/	62	25	7	6	45	/	17.9	7.2	2.0	1.7
	6494	14.45	22.75	39.04	236.4	22.33	1.67	/	65	22	6	7	50	/	25.3	8.6	2.3	2.7
	6495	16.41	20.33	35.04	219.2	19.10	1.08	/	63	22	8	7	40	/	22.1	7.7	2.8	2.4

Notes: I, illite; I/S, illite/montmorillonite mixed-mineral layer; C, chlorite; K, kaolinite; Mixed-mineral layer ratio is the percentage of the montmorillonite crystal layer in a mixed-layer mineral

Caijiapo landslides, they were selected for the case study in which the sampling interval was set as 0.1 m, with the sampling positions shown in Fig. 3d–f.

Thin-section analysis for identifying the mineral and estimating the content in samples from shear zones with different structures was performed in accordance with the national standard: Identification Manual of Transparent Mineral Thin Section and Classification and Nomenclature Schemes of the Rocks—Classification and Nomenclature Schemes of the Sedimentary Rock (GB/T 17412.2 1998).

The quantitative analysis of material composition and pore structure included tests for determining the clay and calcium carbonate content, natural water content, pore ratio, plastic limit, and specific surface area (Table 1). The tests of water content, fine-grained soil particle size, plastic limit, and calcium carbonate content comply with SL-237-002, SL-237-005, and SL-237 in the Standard for Soil Test Method (GB/T 50123 1999). The specific surface area tests conform to the methods outlined in the Determination of the Specific Surface Area of Solids by Gas Adsorption Using the BET Method (GB/T 19587 2004).

The clay mineral content, such as montmorillonite and illite, can be obtained via X-ray diffraction. The hydrologic properties of montmorillonite and those of a mixed-mineral layer of illite and smectite are considerably different, and the hydrologic environment affects the distribution of the aforementioned clay minerals. Three preparation methods were used to analyze 19 triplicated samples. These samples are obtained from the cataclasis, cleavage, and argillation shear zone in landslides, including the Caijiapo, Gaojiaya, and Liujiazhuang landslides (Fig. 3d–f). The first method was used to extract the sample suspension (less than 2 μm) and prepare directional tablets. The second method treated the directional tablets via ethylene glycol saturation. In the third method, the directional tablets were heated for 2 h at 550°C before testing. The X-ray diffraction patterns were determined using the computer information processing software to analyze the quantitative relation between the area of diffraction peak and the clay mineral content, the mineral peak type of a mixed layer, and the mineral ratio of mixed layer and obtain the composition, relative content, and ratio of clay minerals. A Rigaku Rotary Anode X-ray diffractometer (D-Max 2400 Series) running at 12 kW with a tube voltage of 35 Kv, current of 20 mA, stability within +0.03%, focusing area of 0.5 mm (+10 mm), and a goniometer diameter of 185 mm was used to analyze the clay samples. During the experiment, a scanning mode of $2\theta/\theta$ linkage was adopted using a scanning range of 3°–35° and a scanning speed of 2°/min. The testing equipment was a Bruker AXS D8-Focus X-ray diffractometer (the Netherlands). The test procedure complied with the Oil and Gas Industry Standards of the People's Republic of China (SY/T 5163 2010).

The pore structure and hydraulic properties of the shear zone changed gradually with the development of fractures

and shearing planes. The tests were conducted on samples from the undisturbed zone and core zone of the shear zone in the Bojishan landslide to quantitatively measure its pore. First, all the samples would be dried. Then, they would come into contact with water. Next, the amount of water absorbed by the samples will be estimated. Finally, the curves of water absorption in samples were plotted based on the tests. The curves included the water absorption capacity (Q) and water absorption time (t).

The ring shear tests were conducted to simulate the sliding process of the unsaturated samples under undrained conditions and long shear displacement. The average annual rainfall is <700 mm in the northeastern margin of the Tibetan Plateau in China, and the groundwater level changes by 0.2–2.5 m around the shearing zone (e.g., Xin et al. 2016). The landslides are triggered by the rising groundwater level and water pressure (e.g., Xin et al. 2016). However, there is insufficient water for the soil to attain saturated liquefaction at the aforementioned low water pressure. According to the above conditions, two steps were devised in the test for two samples obtained from the borehole ZK2 in Bojishan landslide. First, the natural samples were filled and compressed in the ring shear box for approximately 1 h under 180 kPa and 160 kPa. CO₂ gas was supplied for approximately 1 h to expel ambient air. The initial water pressure was maintained at approximately 10 kPa. Second, the samples were sheared at speeds of 0.02 and 0.05 mm/min. The equipment was a DTA-138 ring shear apparatus (Seiken Inc., Japan).

The residual strength of the samples from the Bojishan landslide could be estimated via repeated shear tests. The test procedure complied with the Standard for Soil Test Method of the People's Republic of China (GB/T 50123 1999).

Results

Reorganized structure of the shear zone

Neogene soft rocks are clastic rocks in which clay minerals, quartz, and mica constitute approximately 80% of the mineral assemblage. In this study, the observed clay content in soft rocks ranged from 20 to 64%. The interaction between clay minerals and water alters the structure of the shear zone. In the fragmentation zone, the soft rock has a blocky structure and is filled with autogenous clasts along the fracture (Fig. 4(a)). In contrast, in the core zone, clay minerals and calcite are aligned in the same direction and have a parallel cleavage domain (Fig. 4(b) and (c)). Clay minerals, such as illite, are arranged in a continuous and directional manner. In the shear zone, there are obvious dispersed water films on the clay minerals, which can be attributed to the interaction of water and rock (Fig. 4(b) and (c)). Under intense deformation episodes, the

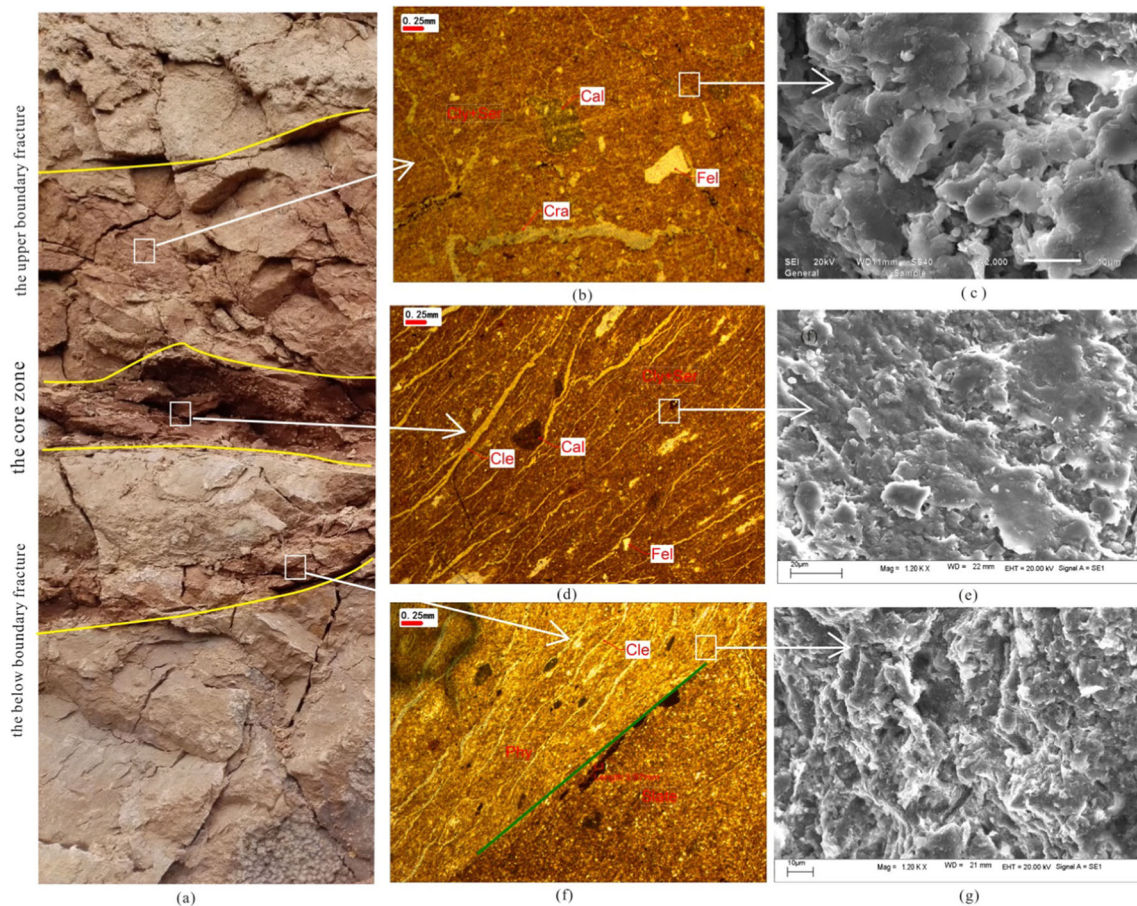


Fig. 4 The structure of shear zone in the Liujiazhuang landslide: (a) Photos of the shear zone; (b–c) the microstructure of the cataclastic layer in upper zone; (d–e) photos of microstructure of the cleavage layer in the core zone; (f–g) photos of microstructure of the argillaceous layer in below zone

platy clay minerals gradually changed from flocculent to scaly and were superimposed.

Distribution characteristics of clay minerals in different structures

The content of clay minerals in the shear zone of short-distance landslides is less than that in case of long-distance landslides. For example, the borehole ZK1 of the Caizigou landslide indicates that the slip zone is cataclastic, and a strong variation zone can be observed at 50.3–51.4 m (Fig. 5a). Two samples from this zone yield total clay contents of 39.64% and 38.42%, with montmorillonite contents of 26.26% and 25.34%, respectively. The measured contents of calcium carbonate are 4.23% and 5.11%, and the specific surface areas relevant to the pore size of rock are 232.74 and 205.66 m²/g (Table 1). The lowest clay mineral content could be observed within the fine particulate matter aggregates on the upper boundary surface of the shear zone (Table 1). The thickness of the sliding zone is approximately 2.1 m in borehole ZK3 of the Xinguncun landslide. The clay mineral contents toward the top, center, and bottom of the sliding zone are 73.39%,

49.85%, and 63.84%, respectively (Fig. 5b). The calcium carbonate contents and montmorillonite concentrations for these sampling positions are 7.86%, 8.83%, and 9.43% and 11.80%, 19.60%, and 12.90%, respectively. In contrast, the montmorillonite content in the core from borehole ZK4, which is within the shear zone of the Xinguncun landslide, is 20.3%.

In case of long-distance landslides, the content of fine particulate matter, such as clay, is slightly greater than that in the vicinity of the core zone, whereas the clay content is the highest in the shear zone and the lowest in the fragmentation zone. In the Bojishan landslide, the depth of the 2.2-m slip zone is 64.4–66.6 m. The upper boundary at 64.4 m is 0.2–0.3-m thick and experiences the greatest deformation. A middle shear plane is defined between 65.2 and 65.6 m with a thickness of 0.4–0.6 m, and a 0.49-m-thick lower boundary can be observed between 65.51 and 66.6 m. The dynamic failure of soft rock affects the clay mineral content. The Bojishan landslide (Fig. 5c) has a clear mechanical structure in which the soft rock in the upper boundary is muddy, the soft rock in the central region contains a shear plane, and the lower boundary displays cleavage. The contents of clay in these

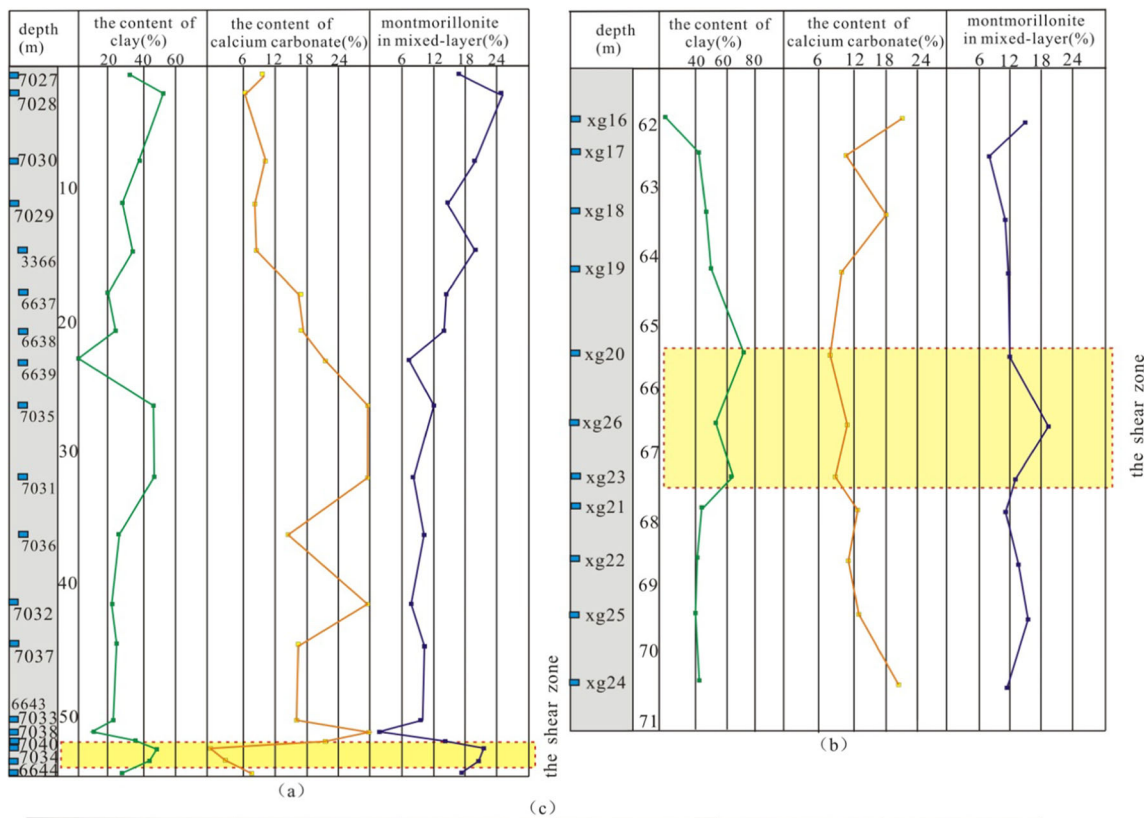


Fig. 5 Characteristics of clay particles in boreholes from geologically young landslides from the northeastern margin of the Tibetan Plateau: **a** borehole ZK1 in Caizigou landslide; **b** borehole ZK3 in Xinguancun landslide; and **c** borehole ZK2 in Bojishan landslide

Table 2 Chemical constituents and groundwater characteristics of the Gaojiaya and Bojishan landslides

Location	pH	Chemical constituents of groundwater (molecule mg/l, denominator meq%)							Salinity (mg/l)	Dry residue (mg/l)	Hydrochemical types
		HCO ₃ ⁻	CO ₃ ²⁻	SO ₄ ²⁻	Cl ⁻	Ca ²⁺	Mg ²⁺	k ⁺ +Na ⁺			
Gaojiaya landslide	7.15	358.15	—	27.65	8.18	75.73	21.06	26.79	338.48	332	HCO ₃ ⁻ -Ca ²⁺ , Mg ²⁺
		87.92		8.62	3.46	56.60	25.95	17.45			
Bojishan landslide	7.51	373.04	—	13.91	13.63	77.82	21.78	25.58	339.24	352	HCO ₃ ⁻ -Ca ²⁺ , Mg ²⁺
		90.07		4.27	5.66	57.21	26.41	16.38			

three regions are 62.60%, 62.46%, and 58.04%, respectively, corresponding to calcium carbonate contents of 1.36%, 1.33%, and 1.18%, respectively. The contents of water in the above three regions are 28.82%, 25.34%, and 25.52%, respectively.

The contents of total clay minerals and montmorillonite are high near the shear surface with cleavage and mud structures, although the calcium carbonate content is visibly low and montmorillonite is concentrated in the upper part of the slip zone. The fragmentation slip zone of the Caijiapo landslide exhibits a thickness of 30 cm and includes a strong fragmentation zone and a disturbance zone. The clay, montmorillonite, and calcium carbonate contents are 50.36%, 25.29%, and 1%, respectively. However, the clay content is 34.08%–39.80%, the montmorillonite content in the mixed-mineral layer is 23.23%–22.78%, and the calcium carbonate content is 2.21%–4.77% within the slide disturbance zone.

The contents of clay minerals, such as montmorillonite and illite, gradually increase because of the hydration reactions (Shuzui 2001; Wen and Aydin 2003). When dynamic fragmentation is strong, the numerous structural planes in the sliding zone promote strong soil–water interaction. The results of a chemical constituent test indicate that the HCO_3^- content is 358.15–373.04 mg/l, SO_4^{2-} content is 13.91–27.65 mg/l, and Ca^{2+} content is 75.73–77.82 mg/l in the Bojishan and Gaojiaya landslides (Table 2). The local groundwater contains high levels of HCO_3^- and Ca^{2+} , providing an environment for the hydration of clay minerals and the conversion reaction of montmorillonite and illite. Shuzui (2001) observed that the stability of kaolinite improved when the concentration of HCO_3^- was as high as 30 mg/L. When the concentration of HCO_3^- exceeded 40 mg/L, the groundwater near the slip surface was in equilibrium with montmorillonite, providing a

favorable environment for the dissolution of kaolinite and formation of montmorillonite. With the increasing HCO_3^- concentration, the active ion exchange of calcium ions was separated, promoting the formation of montmorillonite.

As noted above, the clay minerals in the slip zone primarily contain illite and montmorillonite. The clay mineral content can be identified via X-ray diffraction analysis. Thus, it was determined that the ratio of montmorillonite in mixed-mineral layers near the shear plane is higher than the values obtained for the remaining zones (Fig. 6, Table 1). The clay mineral content and the proportion of montmorillonite in the mixed-mineral layer are 62.60% and 80%, respectively, in the core of the shear zone in the Bojishan landslide, whereas they were 58.04% and 65%, respectively, in other parts of the shear zone. As the shear displacement in the slip zone increases, the proportion of montmorillonite in the mixed-mineral layer gradually increases. The proportion of montmorillonite in the mixed layer of illite and montmorillonite in the Gaojiaya landslide becomes 67%, whereas the absolute content of illite and montmorillonite is 25.5%. In contrast, the montmorillonite in the relatively young Liujiashuang landslide has a maximum value of 55% in the mixed-mineral layer. The amount of montmorillonite in the mixed-mineral layers in the shear zone of these two landslides is lower than that in the shear zone of the Bojishan landslide, indicating that the content of montmorillonite in a landslide shear zone is affected by its dynamic environment.

Change of shear strength

Any change in the mineral composition of the slip zone would affect the permeability of the water within this zone. Water will accumulate or flow in the cracks, pores, and shearing planes under hydrostatic pressure. Pore water penetrates the

Fig. 6 X-ray diffractograms from oriented slides of <2- μm fractions from **a–b** the shear zone of the Caijiapo landslide and **c–d** the shear zone of the Bojishan landslide. ① Normal sample; ② glycolated sample; ③ sample heated to 550°C. I, illite; I/S, illite and montmorillonite mixed-layer; K, kaolinite; C, chlorite; Q, quartz; and Ca, calcium carbonate

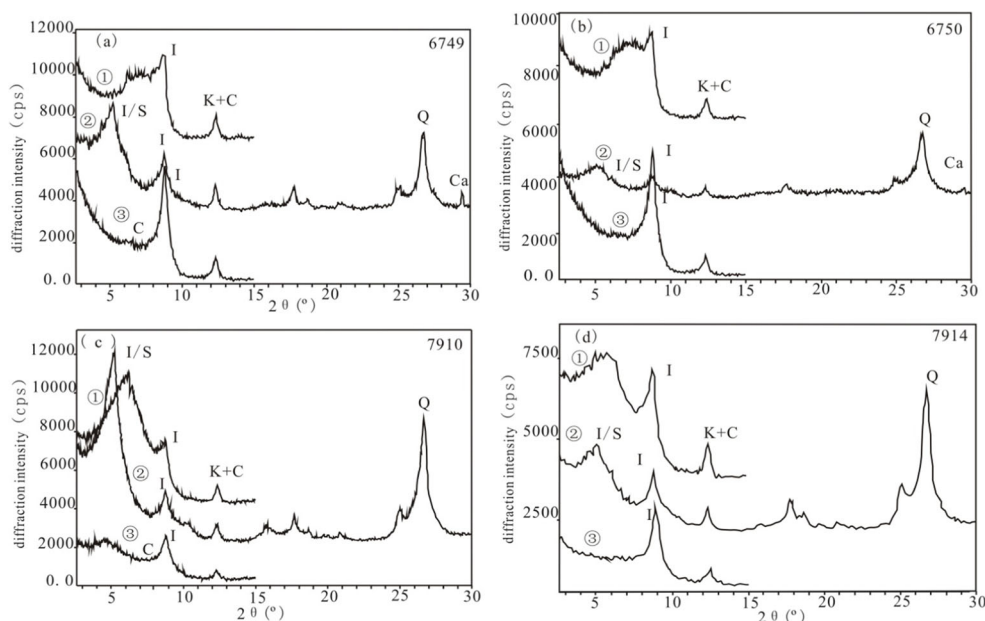
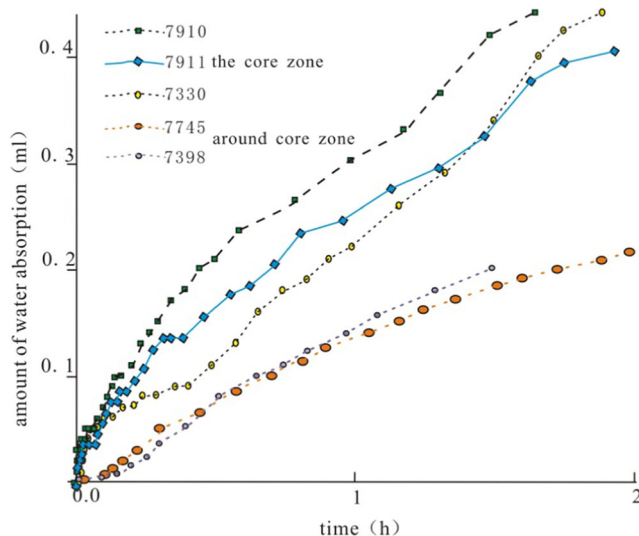


Table 3 Relation between clay content and strength of the shear zone in Bojishan landslide

Sample number	Location	Clay particle content (%)	Water absorption rate (ml/h)	Water content (%)	Residual strength		Steady-state strength	
					Cohesion (kPa)	Internal friction angle (°)	Cohesion (kPa)	Internal friction angle (°)
7910	Core zone	62.6	0.3	28.82	33.46	12.6	25.46	14.5
7911		39.32	0.24	19.98	24.32	9.2	22.11	7.8
7913		62.46	/	18.7	35.28	15.8	/	/
7330		30.69	0.22	22.9	8.29	17.4	/	/
7914		58.04	/	25.1	11.25	16.1	/	/
7915		56.36	/	19.5	24.82	21.5	/	/
7745		Around the core zone	28.68	0.14	19.8	29	22.1	/
7918	47.10		0.13	21.5	20.2	24.8	/	/

fractures when the groundwater pressure increases. The results indicate that absorption rates are 0.24–0.3 ml/h in the shear zones with cleavage and shear planes and 0.13–0.14 ml/h in the fractured zones. Although the soft rock is generally impervious to water, free water will rapidly infiltrate along the shear zones (Fig. 7). The fracture and pore in shear zone would be full of water under high pressure. For instance, the average of pore water pressure in the Bojishan landslide is 92 kPa. The natural water content of the upper boundary in the strong deformation fault is 24.7%–26.8%, that near the middle slide zone is 18.7%–22.9%, and that near the lower surface is only 18.7%–25.1% (Table 3). The dilatancy and grain crushing in shear zone are the main reasons for the increase of cracks and pores (Muhammad et al. 2004).

The seepage of water and its interaction with minerals can be attributed to the development of the shearing surfaces. Usually, the undisturbed soft rock is not conducive to the flow of water. The change in volume of soft rock occurs in three

**Fig. 7** Water absorption–time curve of the slip zone and the surrounding rock for samples from the Bojishan landslide

different stages when it is compressed and sheared. In the first stage, the samples are compressed; this is accompanied by an increase in pore water pressure. In the second stage, the pore water pressure gradually decreases to negative values accompanied by a gradual decrease in shear stress. In the third stage, the pore water pressure progressively increases and subsequently experiences another reduction (Fig. 8).

The accumulation of shear deformation and water could change the strength of the soft rock. The core of the shear zone has a high natural water content. The internal friction angle at the upper boundary of the fault, that of the main slip zone in the central zone, and that of the lower boundary fault are estimated to be 9.2°–12.6°, 15.8°–17.4°, and 15.8°–16.1°, respectively, through repeated tests of the undisturbed samples from the shearing zones in the Bojishan landslide (Table 3).

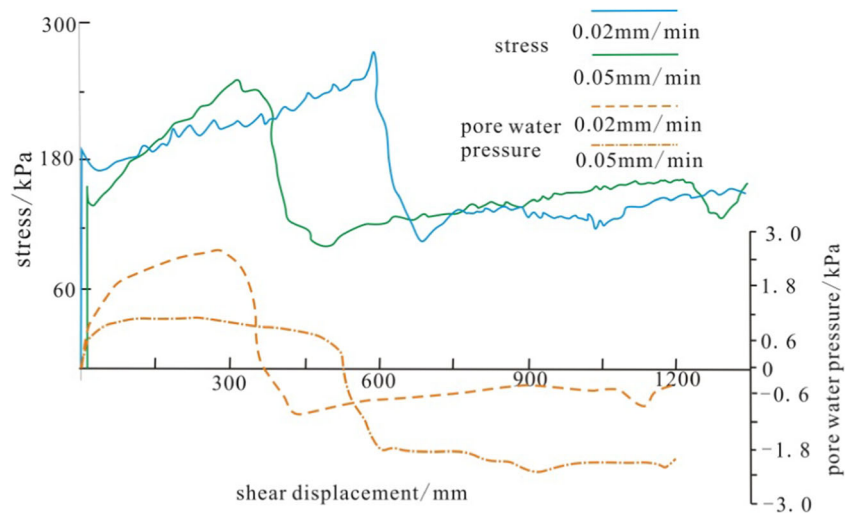
Discussion

The distribution of montmorillonite in shear zones is not uniform, and clay particles can be observed as aggregates along the fracture surface. The cataclasis of Neogene soft rock results in a gradual transformation of the materials in the shear zone through fragmentation, formation of cleavage, plasticization, argillation, and the accumulation of clay particles (Wu et al. 2020). The argillaceous layer has the lowest residual strength because it contains the most number of cracks and exhibits the lowest water content. However, it remains unclear which processes cause the accumulation of mixed-mineral layers and which processes are responsible for the notable increase in montmorillonite content near the shear surface.

Relation between the structure and clay minerals

The coarse and fine particles within the shear zone segregated during motions, and a parallel orientation structure developed

Fig. 8 Ring shear tests for samples 7910 and 7911 from the borehole ZK2 in the Bojishan landslide



during the steady-state deformation (Muhammad et al. 2004). According to the data from the rock samples obtained from the Longzhong Basin (Table 4), water content near the shear surface varies from 10.12 to 19.75%, and the average content of montmorillonite is 13.26%, with a maximum of 23.74%. The average ratio of illite–montmorillonite mixed-mineral layer in these mudstones is 38%, with the highest clay and internal water content of 65.23% and 14.53%, respectively (Table 4).

Based on statistical analysis, higher clay contents tend to correspond to higher mixing layer ratios in the sliding zone. The illite/montmorillonite mixed-mineral layer that accumulates near the shear surface exhibits strong hydrophilicity (Fig. 9). The clay contents in the argillation layer reach 62%, and

the water content exceeds the plastic limit at 28.82%. The mixed-mineral layer ratio ranges from 80 to 100%; however, the mixed-mineral layer ratio in the unaffected original soft rock is only 50%. Thus, as noted above, soft rock is originally impervious to water; however, it can be easily infiltrated in the post-slide state.

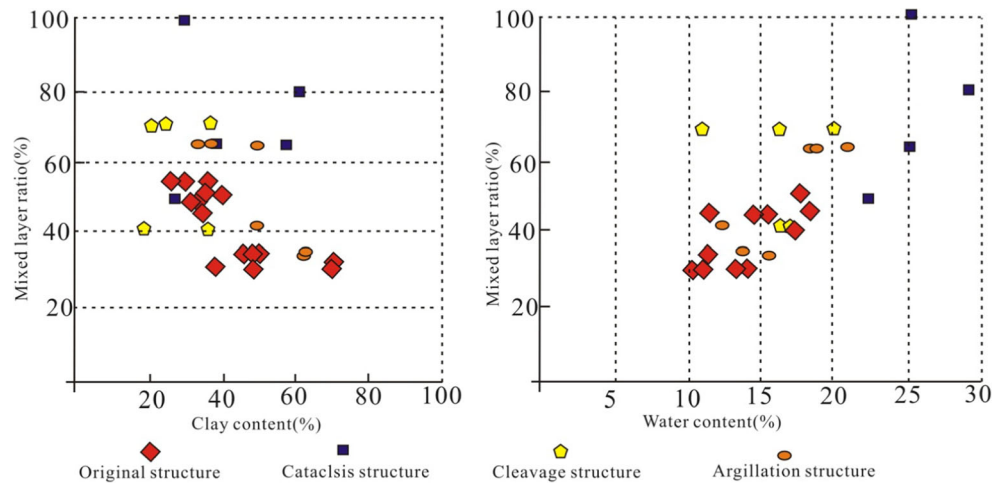
The arrangement of minerals and particles in the shear zone are controlled by physical friction. In the cleavage zone, fine and delicate clayey particles are arranged in an orderly network. Den Brok (1998) concluded that compression through pressure dissolution is an important factor associated with cleavage formation. Pressure dissolution can be observed at the boundary of particles in the direction of maximum

Table 4 Clay mineral content in the shear zones in northwestern China

Location	Sampling number	Montmorillonite in mixed-layer (%)	Content of calcium carbonate (%)	Water content (%)	Content of clay (%)	Relative content of clay minerals (%)				Mixed-mineral layer ratio (%)	Absolute content of clay minerals (%)			
						I/S	I	K	C		I/S	I	K	C
Guanzhong Basin	5479	23.74	6.32	/	32.99	72	17	7	4	45	23.75	5.61	2.31	1.32
	5480	21.44	7.99	18.15	36.08	72	19	6	3	45	25.98	6.86	2.17	1.08
	5483	20.02	6.64	/	31.87	69	21	6	4	40	21.99	6.69	1.92	1.28
	5484	18.49	9.00	19.75	28.99	62	25	7	6	45	17.97	7.25	2.03	1.74
	5495	19.10	1.08	18.18	35.04	63	22	8	7	40	22.08	7.71	2.80	2.45
Longzhong Basin	7001	14.32	6.48	10.12	64.59	38.5	45.2	0	16.3	35	24.87	18.02	0	10.53
	7002	13.26	19.05	11.53	39.87	34.5	47.3	0	18.2	30	13.76	17.13	0	7.26
	7003	13.64	39.06	11.88	36.22	40.0	48.6	0	11.4	45	14.49	31.70	0	4.13
	7004	14.37	13.71	14.53	65.23	31.8	56.8	0	11.4	30	20.74	38.52	0	7.44
Xining Basin	6619	18.15	7.28	15.76	35.36	48	38	5	9	45	17.0	13.4	1.8	3.2
	6621	13.99	12.83	13.69	31.88	68	19	5	8	45	21.7	6.1	1.5	2.6
	6622	16.40	15.68	11.91	33.76	46	38	6	10	45	15.5	12.8	2.0	3.4
	6628	16.15	2.52	14.16	44.44	66	26	3	5	30	29.3	11.6	1.3	2.2

Notes: I, illite; I/S, illite/montmorillonite mixed-mineral layer; C, chlorite; K, kaolinite; Mixed-mineral layer ratio is the percentage of the montmorillonite crystal layer in a mixed-mineral layer

Fig. 9 Relation between the mixed-mineral layer ratio and clay particle content (a) and water (b)



vertical compression. The dissolved substances migrate and accumulate from the area with the higher chemical potential energy to the low-stress region. Because quartz and feldspar dissolve in the direction of vertical compression, their particles

become lenticular or form long strips. Pressure dissolutions continuously progress on the boundary of the particles or the interface of layers in the direction of vertical compression. Insoluble residues, such as clay or mica, become enriched,

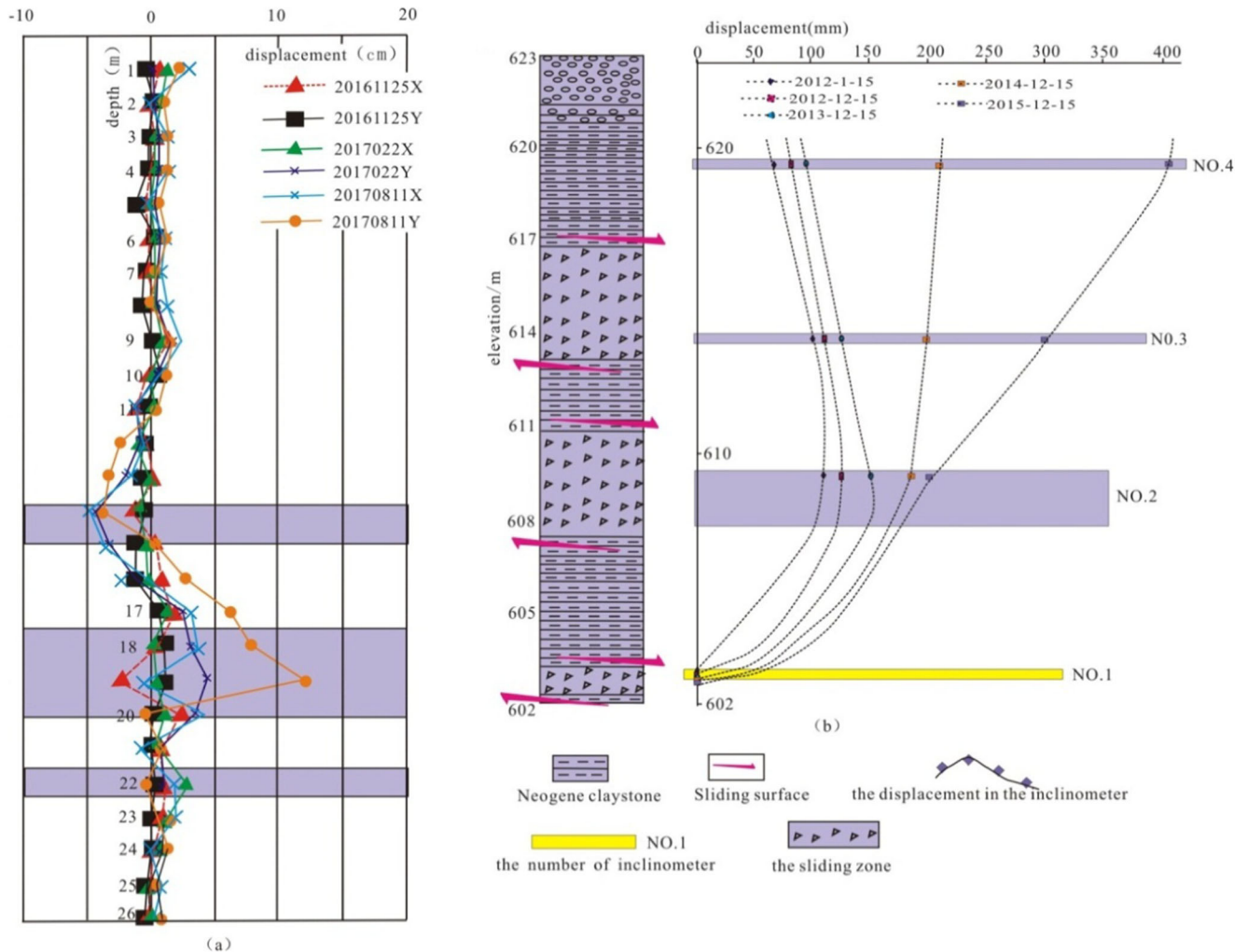


Fig. 10 Variations in displacement landslides: **a** displacement of the Hongluocun landslide from 2016 to 2017 and **b** displacement of the shear zone in the Bojishan landslide from 2012 to 2015

and the sheet minerals, such as mica, progressively rotate and align in the direction of maximum vertical compression, forming cleavage domains.

The deformation of shear zone

The penetration of water would induce soil–water interaction along shear plane. The deformation of the shear plane primarily includes creep and rapid slip stages. The creep stage is dominated by viscous deformation, as indicated by the continuous creep slip of the Hongluo Village landslide in Tianshui from 2016 to 2017 (Fig. 10a). The upper boundary fault plane of the horizontal slip zone varies most intensely, and its cumulative displacement is the largest. In the Bojishan landslide from 2012 to 2016, the cumulative displacements of the #2 and #3 main sliding zones were 150.73 and 152.05 mm, whereas those of the #1 lower fracture surface and #4 upper fracture surface were 0 and 99.75 mm, respectively (Fig. 10b). The rapid slip of the shear zone extends along the upper shear plane. In addition, the clay mineral content tends to be the largest in zones with the maximum displacement (Massey et al. 2013, 2016; Petley et al. 2002; Palladino and Peck 1972). The fracture in the clay-rich soft rock allowed the shear plane to become a pathway for free water; thus, there is a relation between physical mechanisms and the rock–water chemical reactions of clay that should be addressed in future studies.

Conclusions

In this study, seven landslides were selected to analyze the structural development process of shear zone. Several vertical profiles were quantitatively studied from top to bottom in terms of the material composition, pore structure, and water content to understand the changes in the cementation and frictional properties of the shear zone. Even though no sliding surface liquefaction occurred, the slipping of clayey particles could be observed.

The shear zones are characterized with layers exhibiting cataclasis, cleavage, and argillation in the core. With the increasing displacement of the shear zone, the clay particles accumulate in the core of the shear zone, surrounded by the remaining mineral particles. Montmorillonite aggregates can be observed along the shear boundaries of the shear surface. The montmorillonite content is the highest near the core zone. The differences in montmorillonite content in the three fracture surfaces in the shear zone can be attributed to their varying cumulative displacements.

Funding This study was supported by the National Natural Science Foundation of China (Grant No. 42077276) and the Geological Survey Project (No. DD20190717).

References

- Carey JM, Petley DN (2014) Progressive shear-surface development in cohesive materials; implications for landslide behaviour. *Eng Geol* 177:54–65
- Caterina DM, Roberto V, Margherita V, Pascale S, Sdao F (2010) Structure and kinematics of a landslide in a complex clayey formation of the Italian Southern Apennines. *Eng Geol* 116:311–322
- Caterina DM, Roberto V, Margherita V (2013) Plastic and viscous shear displacements of a deep and very slow landslide in stiff clay formation. *Eng Geol* 162:53–66
- Den Brok SWJ (1998) Effect of microcracking on pressure-solution strain rate: the Gratz grain-boundary model. *Geology* 26(10):95–98
- GB/T 17412.2 (1998), Identification Manual of Transparent Mineral Thin Section and Classification and Nomenclature Schemes of the Rocks—Classification and Nomenclature Schemes of the Sedimentary Rock. National standards of the People's Republic of China.
- GB/T 19587 (2004), Determination of the Specific Surface Area of Solids by Gas Adsorption Using the BET Method. National standards of the People's Republic of China.
- GB/T 50123 (1999), the Standard for Soil Test Method. National standards of the People's Republic of China.
- Hart MW (2000) Bedding parallel shear zones as landslides mechanisms in horizontal sedimentary rocks. *Environ Eng Geosci* 2:95–113
- James VH (2001) Discussion on “bedding parallel shear zones as landslides mechanisms in horizontal sedimentary rocks.”. *Environ Eng Geosci* 2:217–219
- Lupini JF, Skinner AE, Vaughan PR (1981) The drained residual strength of cohesive soils. *Geotechnique* 31(2):181–213
- Massey CI, Petley DN, Mcsaveney MJ (2013) Patterns of movement in reactivated landslides. *Eng Geol* 159:1–19
- Massey CI, Petley DN, Mcsaveney MJ, Archibald G (2016) Basal sliding and plastic deformation of a slow, reactivated landslide in New Zealand. *Eng Geol* 208:11–28
- Muhammad WA, Kyoji S, Hiroshi F, Wang G (2004) Evolution of shear-zone structure in undrained ring shear tests. *Landslides* 1:101–112
- Palladino DJ, Peck RB (1972) Slope failures in an overconsolidated clay, Seattle, Washington. *Geotechnique* 22(4):563–595
- Petley DN, Bulmer MH, Murphy W (2002) Patterns of movement in rotational and translational landslides. *Geology* 30:719–722
- Picarelli L, Comegna L, Tommasi P (2006) Discussion to “evolution of shear zone structure in undrained ring-shear tests” by M.W. Agung, K. Sassa, H. Fukuoka, and G. Wang [Landslides 1(2):101–102, July 2004]. *Landslides* 3:265–268
- Shuzui H (2001) Process of slip-surface development and formation of slip-surface clay in landslides in tertiary volcanic rocks, Japan. *Eng Geol* 68:289–317
- Skempton AW (1970) First-time slides in over-consolidated clays. *Geotechnique* 20(3):320–324
- Skempton AW (1985) Residual strength of clays in landslides, folded strata and the laboratory. *Geotechnique* 35(1):3–18
- SY/T 5163 (2010), Analysis method for clay minerals and ordinary non-clay minerals in sedimentary rocks by the X-ray diffraction. Oil and Gas Industry Standards of the People's Republic of China.
- Wang F, Kyoji S, Hiroshi F (2000) Relationship between grain crushing and excess pore pressure generation by sandy soils in ring shear tests. *J Nat Dis Sci* 22(2):87–96
- Wen BP, Aydin A (2003) Microstructural study of a natural slip zone, quantification and deformation history. *Eng Geol* 68:289–317
- Wu Q, Jiang Y, Tang H, Luo H, Wang X, Kang J, Zhang S, Yi X, Fan L (2020) Experimental and numerical studies on the evolution of shear behaviour and damage of natural discontinuities at the interface between different rock types. *Rock Mech Rock Eng* 53:3721–3744

- Xin P, Liang CY, Wu SR, Liu Z, Shi JS, Wang T (2016) Kinematic characteristics and dynamic mechanisms of large-scale landslides in a Loess Plateau: a case study for the north bank of the Baoji stream segment of the Wei River, China. *Bull Eng Geol Environ* 75:659–671
- Xin P, Liu Z, Wu S, Liang C, Cheng L (2018) Rotational-translational landslides in the Neogene basins at the northeast margin of the Tibetan Plateau. *Eng Geol* 244:107–115
- Yenes M, Monterrubio S, Nespereira J, Santos G (2009) Geometry and kinematics of a landslide surface in tertiary clays from Duero Basin (Spain). *Eng Geol* 104:41–54
- Yenes M, Monterrubio S, Nespereira J, Santos G, Fernandez-Macarro B (2015) Large landslides induced by fluvial incision in the Cenozoic Duero Basin (Spain). *Geomorphology* 246:263–276